PHYSICAL REVIEW A VOLUME 21, NUMBER 4 APRIL 1980

High-precision laser-rf double-resonance spectroscopy of the $^2\Sigma$ ground state of CaF

W. J. Childs and L. S. Goodman
Argonne National Laboratory, Argonne, Illinois 60439

(Received 20 November 1979)

The laser-rf double-resonance technique has been applied to achieve high-precision measurements of the N dependence of the spin-rotation and hyperfine interaction in the $^2\Sigma(v''=0)$ ground state of CaF in a molecular beam. The effective spin-rotation-interaction constant is shown at small N to depart markedly from the asymptotic value found at large N, and the average hfs splitting of the $J''=N+1/2$ and $J''=N-1/2$ levels is shown to exhibit a maximum for $N=11$–12. These newly observed effects, though consistent with the theory, have not been explicitly predicted previously.

I. INTRODUCTION

A considerable amount of high-resolution spectroscopic work in recent years has been directed toward the systematic understanding of the structure of selected diatomic molecules.[1-7] Line by line analysis, in particular, has been extremely valuable for the interpretation. In several studies,[1,3,5] laser-induced flourescence and microwave-optical double resonance (MODR) have been combined, with the result that most of the structural constants of the molecules studied could be accurately evaluated. The resolution achieved in the fluorescence studies, however, has been limited by Doppler broadening in the vapor, and the linewidths observed in MODR, though much smaller than those of the fluorescence lines, still suffer from Zeeman splitting, pressure broadening, and microwave power saturation.[3] As a result, the hyperfine structure (hfs) is normally unresolved, and in addition, measurement of the spin-rotation interaction is of limited precision.

The molecular-beam, laser-rf double-resonance technique used in the present experiment was devised in 1975 by Rosner, Holt, and Gaily,[8] and independently by Ertmer and Hofer;[9] it appears to be ideally suited to supplement the MODR technique to yield molecular spin-rotation and hfs data of much higher precision. As will be discussed below, spin-rotation splittings and hfs can be measured for the molecular ground state to a precision of 1 kHz or less. The sensitivity of the new method is also extremely high.

The choice of CaF for examination by the laser-rf double-resonance technique was the result of a suggestion by Renhorn,[10] who pointed out that the extensive laser fluorescence and MODR results of Nakagawa *et al.*[4,5] would be extremely valuable as a guide. Renhorn also pointed out that some new features might be observed if the spin-rotation and hfs interactions could be observed with linewidths much smaller than those previously attained.

II. METHOD

Although the present laser-rf double-resonance technique was first applied to sodium dimers,[8] its principal application to date has been to studies of atomic hyperfine structure. Since the technique has been described[8,9,11] several times in the literature, only a brief description will be given here. A collimated molecular beam is intersected orthogonally by the single-frequency beam of a tunable cw dye laser. In the present application, the laser is tuned to excite CaF molecules from a particular level of the $^2\Sigma$ ground state (with specified vibrational, rotational, and hfs quantum numbers) to an appropriate $^2\Pi_{1/2}$ excited-state component. The particular lines used in the present experiment were the $P_1(J'')$ lines from the $J''=N+\frac{1}{2}$, $F''=J''\pm I$ $(I=\frac{1}{2})$ levels of $^2\Sigma_{1/2}$, $v''=0$ to $J'=N-\frac{1}{2}$, $F'=J'\pm I$ levels of $^2\Pi_{1/2}$, $v'=0$ as shown in Fig. 1. After the molecules have traversed the laser beam, very few remain in the particular hfs component of the $J''=N+\frac{1}{2}$ level used. For this reason, if a second laser beam, identical in frequency to the first, is used to probe the molecular beam still further from the beam source, very little fluorescence can be produced unless the depleted lower level can be repopulated in the space between the two laser interaction regions. This can be accomplished by inducing magnetic-dipole transitions within the N manifold. Such transitions are in the frequency range $0<\nu<5$ GHz for $0\leq N\leq 100$ in CaF. When the rf is tuned to such a resonance, the increase in fluorescence can be many times the background counting rate, rather than the 1–2% increase reported[5] as typical for a MODR experiment. In addition to the very high sensitivity attainable, very narrow linewidths are obtained. Since rf transitions occur within the lower electronic (ground) state, and many cm from either laser interaction region, the lifetime of the upper, $^2\Pi$ level and the linewidth of the laser do not affect the observed linewidth; it is determined only by the transit time

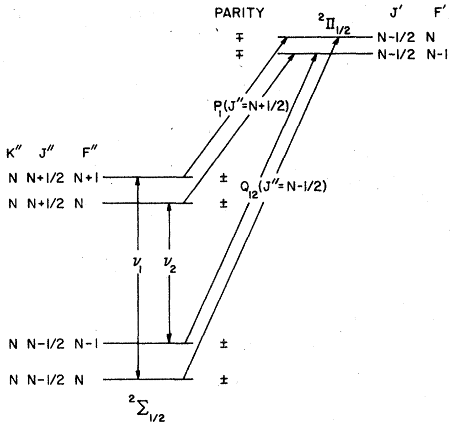

FIG. 1. Detail of the $(v''=0)\,^2\Sigma$ energy levels for a given N, showing the $P_1(J'')$ and $Q_{12}(J''-1)$ transitions to the $^2\Pi_{1/2}$ state, and two magnetic-dipole rf transitions that can be observed by the laser-rf double-resonance technique. The ground-state spin-rotation interaction and the average hfs splitting can be evaluated from ν_1 and ν_2. Any possible hyperfine structure in the upper ($^2\Pi$) state cannot affect the rf transitions.

of the molecule through the rf region and by a small Zeeman broadening due to any residual magnetic field. In the present apparatus, in which magnetic shielding is used to reduce the field to a few mG, the typical full width at half maximum (FWHM) observed is 10–40 kHz. It should be emphasized that any rf transitions observed with the present arrangement are necessarily in the lower (ground) electronic state, since the lifetime of the upper state is too short to allow excited molecules to reach the rf-field region.

III. APPARATUS

Details of the present apparatus, and a more complete description of the method as applied to an atomic beam, have been previously published.[11] The oven used as the beam source for CaF was a hollow tantalum cylinder 1.5 cm high and 0.8 cm in diameter, with a 1-mm hole through the top lid. It was loaded with a charge of CaF_2 powder and some chips of calcium metal and heated with about 120 W of electron-bombardment power. One such charge usually lasted for about three hours of operation.

The only other departure from the previously described setup was the use of an interferometric "λ-meter", built by Lee,[12] which measured the wavelength (in air) of the dye laser by comparison with a He-Ne (6328- Å) standard using fringe-counting techniques. Although the instrument is still in a preliminary stage, a precision of ±0.01 Å is routinely achieved. This instrument was absolutely essential to the success of the experiment.

IV. DOPPLER-FREE LASER-FLUORESCENCE SPECTROSCOPY

Before the laser-rf double-resonance technique could be applied, it was necessary to obtain complete fluorescence spectra, and to identify all the observed lines uniquely. The $P_1(J'')$, $Q_{12}(J'')$ series of the v'', $v'=0$ band of the $^2\Pi_{1/2} \rightarrow {}^2\Sigma_{1/2}$ transition were selected for the first studies. The wavelength of the bandhead had been previously measured by Nakagawa *et al.*[5] to be at 6064.40 Å, and Fig. 2 shows the result of a laser scan through

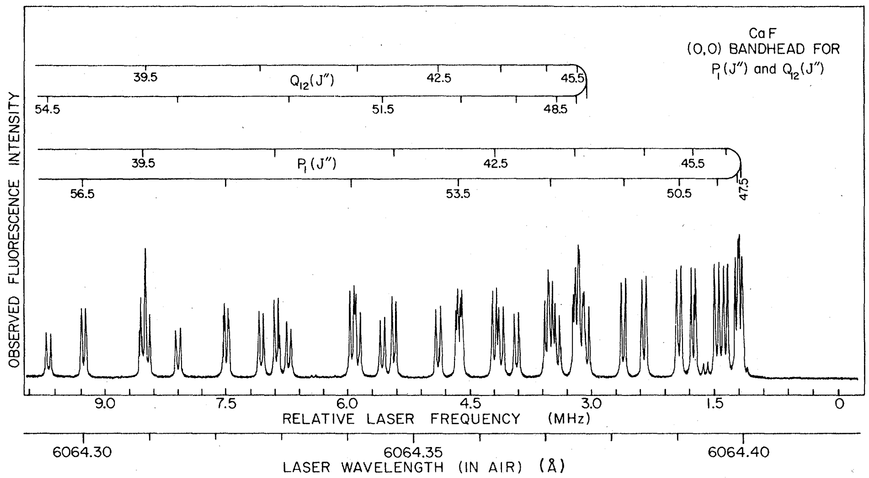

FIG. 2. A small portion of the observed $^2\Pi_{1/2} \longleftrightarrow {}^2\Sigma_{1/2}$ spectrum in the vicinity of the (0, 0) bandhead at 6064.40 Å. Although the wavelength scale is only accurate to about ±0.005 Å, the 10-mK (300-MHz) frequency markers provided are accurate to better than 1%. Each line is split by the hyperfine interaction into two components $[I(^{19}F)=\frac{1}{2}]$, each with a linewidth of about 20 MHz. A key above the spectrum identifies all the strong lines.

this region. The observed fluorescence intensity (over a broad wavelength region including the laser wavelength) is plotted as a function of the exciting laser wavelength, and markers every 10 mK (300 MHz), from a 25-cm confocal Fabry-Perot, are shown. The wavelengths shown are calculated from these markers and an accurate λ-meter measurement of the position of the bandhead; the wavelength scale has an absolute accuracy of about ±0.005 Å.

The most notable feature of the spectrum shown, apart from the very high resolution (the observed FWHM is ~20 MHz), is the splitting of every line into two hfs peaks, about 47–55 MHz apart $[I(^{19}F)=\frac{1}{2}]$. The separate bandheads of the P_1 and Q_{12} series are also clear. The spectrum shown represents less than 4% of the high-resolution spectra obtained for the (0,0) band; 0.1 Å out of the 2.8 Å scanned.

For the initial identification of the individual lines, the data published by Nakagawa *et al.*[5] proved to be of immense value. Although they were unable to resolve $P_1(J'')$ from $Q_{12}(J''-1)$ at small J'', the lumped lines they saw formed a series whose members were separated from each other by about 0.09 Å for J'' values near 10.5. Since the absolute precision of the λ-meter in its present form is 0.01 Å, comparison of the new, much-higher-resolution data with that of Nakagawa *et al.*[5] in this region allowed a unique identification of the observed lines. It was then possible, by using the Nakagawa[5] Hamiltonian and their deduced molecular constants, to identify nearby members of the P_1 and Q_{12} series, and ultimately to count and identify, line by line, all the members from $J''=1.5$ through 92.5. At the very highest $J''\gtrsim 85.5$ and lowest $J''\lesssim 7.5$, identification was in some cases difficult because of the presence of the (1,1) band and because of reduced intensities. The identification of the individual components was confirmed by rf studies, as discussed below. Table I lists the observed wavelengths of the $P_1(J'')$ and $Q_{12}(J'')$ series to an accuracy of ±0.01 Å.

TABLE I. Measured values of the wavelength, in air, for the $P_1(J'')$ and $Q_{12}(J'')$ lines of the (0,0) band of the $^2\Pi_{1/2} \longleftrightarrow {}^2\Sigma_{1/2}$ transition in CaF. The wavelengths were measured to ±0.01 Å interferometrically by comparison with a 6328-Å He-Ne laser standard. The data of this table are plotted in Fig. 3.

	Observed wavelength (Å) (air)			Observed wavelength (Å) (air)	
J''	$Q_{12}(J'')$	$P_1(J'')$	J''	$Q_{12}(J'')$	$P_1(J'')$
1.5	6061.80	6061.70	47.5	64.38	64.40
2.5	61.91	61.80	48.5	64.37	64.40
3.5	62.01	61.91	49.5	64.37	64.40
4.5	62.12	62.01	50.5	64.36	64.39
5.5	62.22	62.12	51.5	64.35	64.39
6.5	62.34	62.22	52.5	64.33	64.38
7.5	62.44	62.34	53.5	64.32	64.35
8.5	62.55	62.45	54.5	64.30	64.34
9.5	62.63	62.55	55.5	64.28	64.33
10.5	62.71	62.64	56.5	64.26	64.31
11.5	62.81	62.72	57.5	64.23	64.28
12.5	62.90	62.82	58.5	64.20	64.26
13.5	62.97	62.90	59.5	64.16	64.23
14.5	63.06	62.98	60.5	64.13	64.19
15.5	63.14	63.07	61.5	64.09	64.15
16.5	63.22	63.15	62.5	64.06	64.13
17.5	63.29	63.23	63.5	64.01	64.08
18.5	63.37	63.30	64.5	63.96	64.04
19.5	63.45	63.38	65.5	63.91	64.00
20.5	63.51	63.45	66.5	63.84	63.94
21.5	63.56	63.51	67.5	63.80	63.89
22.5	63.63	63.58	68.5	63.74	63.83
23.5	63.69	63.64	69.5	63.68	63.80
24.5	63.75	63.71	70.5	63.61	63.72
25.5	63.80	63.77	71.5	63.55	63.64
26.5	63.85	63.82	72.5	63.49	63.58
27.5	63.91	63.87	73.5	63.42	63.51
28.5	63.96	63.92	74.5	63.34	63.45
29.5	64.01	63.97	75.5	63.26	63.38
30.5	64.06	64.02	76.5	63.17	63.29
31.5	64.09	64.06	77.5	63.09	63.21
32.5	64.13	64.11	78.5	63.00	63.13
33.5	64.16	64.14	79.5	62.92	63.05
34.5	64.19	64.17	80.5	62.83	62.95
35.5	64.22	64.20	81.5	62.72	62.88
36.5	64.25	64.23	82.5	62.64	62.77
37.5	64.28	64.27	83.5	62.55	62.69
38.5	64.30	64.29	84.5	62.44	62.58
39.5	64.32	64.31	85.5		62.48
40.5	64.33	64.33	86.5	62.20	62.38
41.5	64.35	64.35	87.5	62.09	62.26
42.5	64.36	64.36	88.5	61.97	62.13
43.5	64.36	64.38	89.5	61.87	62.02
44.5	64.37	64.39	90.5	61.75	61.90
45.5	64.38	64.39	91.5	61.62	61.79
46.5	64.38	64.40	92.5		61.68

The identification of the lines in the small part of the spectrum shown in Fig. 2 is given above the lines. As one follows either the $P_1(J'')$ or $Q_{12}(J'')$ series from J'' values of 39.5 to 54.5, one sees that the bandhead occurs for $N=47$. The measured wavelengths of all the members observed in these series are shown in Fig. 3 as a function of the J'' values. The near coincidence of the $Q_{12}(J''-1)$ and $P_1(J'')$ lines at small J'' is gradually upset as J'' increases and the spin-rotation interaction (proportional to J'') grows. Figure 3 should not be used to infer the spin-rotation splittings, however, since the position of every line was determined by an independent λ-meter reading accurate only to ±0.01 Å. The individual spectra, exemplified by Fig. 2, give much higher precision (to better than 1%) values for these splittings by comparison with the Fabry-Perot fringes. These re-

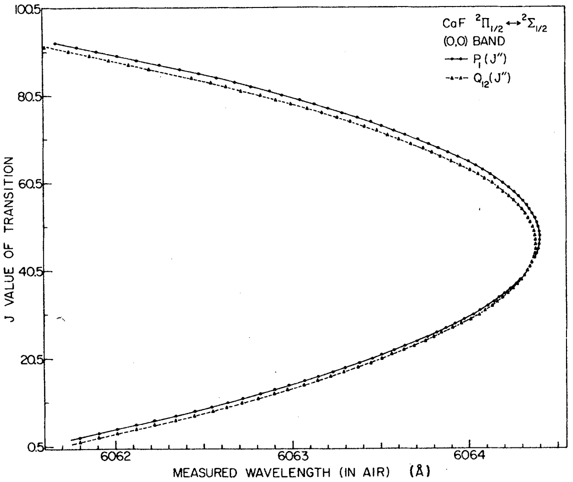

FIG. 3. Plot of the observed wavelengths for the $P_1(J'')$ and $Q_{12}(J'')$ lines against J''. The wavelengths plotted were measured independently for each line to ±0.01 Å by the interferometric λ meter described in the text. The spacings between particular lines of interest were determined not from these wavelength measurements, but by comparison with the fringes of a 25-cm confocal Fabry-Perot interferometer, and in some cases by the laser-rf double-resonance technique as described in the text.

sults will not be tabulated, however, since the radio-frequency data give the same information thousands of times more precisely still. The laser fluorescence spectra also give the hfs splittings of the $P_1(J'')$ and $Q_{12}(J'')$ lines, although the precision is only about 4–5 MHz, or 10%. The average hfs splitting for a given N of the $^2\Sigma(v''=0)$ ground state is given precisely by the rf work; these results are not affected by possible hfs or other features of the $^2\Pi$ upper state. The rf results will be presented below.

V. LASER-RF DOUBLE-RESONANCE SPECTROSCOPY

Since the two transitions labeled ν_1 and ν_2 in Fig. 1 involve flipping primarily an electron spin, they can be expected to have transition probabilities comparable to the magnetic-dipole transitions between adjacent hfs levels of an atom. Direct observation of the hfs splittings within the $J''=N+\frac{1}{2}$ and $N-\frac{1}{2}$ states, however, involve flipping primarily a nuclear magneton, and can therefore be expected to be very much weaker.[13]

In making the double-resonance measurements of ν_1 or ν_2 for a particular N, care has to be taken to be sure the laser was depleting the population of the appropriate hfs level. Thus the red (longer-wavelength) hfs component of $P_1(J'')$ was used when measuring ν_1, and the blue component when measuring ν_2. If the $Q_{12}(J''-1)$ line had been used instead, the ordering would be reversed. A typical result is shown in Fig. 4, which depicts a radio-frequency scan through ν_1, with the laser tuned to the red hfs component of $P_1(16.5)$. The FWHM is 22 kHz, and the line center is easily determined to ±1 kHz or about 1 ppm. Although the linewidth can be affected by application of too much rf power, the position of the line center is very insensitive to the power level used.

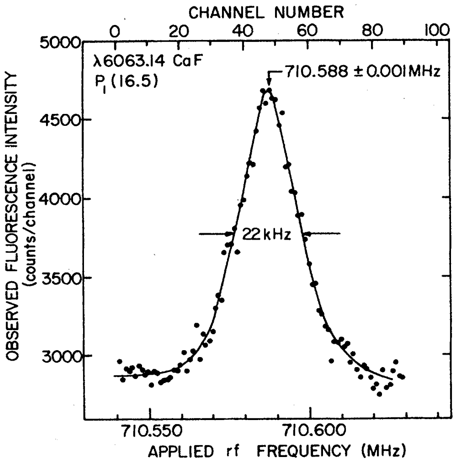

FIG. 4. Radio-frequency scan through the transition ν_1 for $N=16$. The observed fluorescence intensity is plotted as a function of the applied radio frequency. The linewidth (FWHM = 22 kHz) results partly from transit time of the molecules through the rf region, and partly from a slight Zeeman broadening due to the residual magnetic field of a few mG.

Thus for each value of N studied by double resonance in the P_1, Q_{12} series, the two rf frequencies ν_1 and ν_2 were obtained with high precision (the information is summarized in Table II). The experimental uncertainties in ν_1 and ν_2 are about 2 in the last decimal. (Much greater precision can be achieved by the laser-rf double-resonance technique if standard techniques of atomic-beam magnetic resonance, including the Ramsey separated-oscillatory-field method,[14] are employed.)

From the two frequencies observed, two parameters can be evaluated as functions of N, the ground-state rotational quantum number. We define the effective ground-state spin-rotation interaction constant γ'' to be

$$\gamma'' = \frac{\nu_1+\nu_2}{2N+1} \tag{1}$$

and the average hfs splitting $\langle\Delta\nu\rangle$ of the $J''=N+\frac{1}{2}$ and $N-\frac{1}{2}$ states as

$$\langle\Delta\nu\rangle = \tfrac{1}{2}(\nu_1-\nu_2). \tag{2}$$

Figure 5 shows the experimental value of γ'' plotted against N. Although the value is constant

TABLE II. Observed transition frequencies, as identified in Fig. 1, for different values of the rotational quantum number N in the $^2\Sigma$ ($v''=0$) ground state of CaF, as determined by the laser-rf double-resonance technique. The experimental uncertainties are about ±2 in the last decimal. The effective ground-state spin-rotation-interaction constant γ'', and the average hfs splitting of the $J''=N+\frac{1}{2}$ and $N-\frac{1}{2}$ levels, as deduced from the measured resonance frequencies, are also listed as functions of N. The strong dependence of γ'' and $\langle\Delta\nu\rangle$ on N has not been observed before.

N	ν_1 (MHz)	ν_2 (MHz)	γ'' (MHz)	$\langle\Delta\nu\rangle$ (MHz)
3	211.974		45.2 [a]	
6	322.41	214.18	41.276	54.115
8	398.850	290.552	40.553	54.149
9	437.447	329.130	40.346	54.155
10	476.208	367.881	40.195	54.164
11	515.088	406.764	40.081	54.162
12	554.070	445.735	39.992	54.168
14	632.230	523.910	39.867	54.160
16	710.588	602.289	39.784	54.150
29	1222.038	1114.016	39.594	54.011
46	1892.786	1785.418	39.551	53.683
66	2682.843	2576.620	39.545	53.112
83	3354.534	3249.616	39.546	52.459

[a] The rough γ'' value given for $N=3$ follows from the measured value of ν_1 and an extrapolated value of $\langle\Delta\nu\rangle$ from Fig. 6.

at large N as expected, it departs strikingly from constancy at small values of N. It may be noted that the extreme constancy determined for γ'' at large N, as shown in Fig. 5 and Table II, is quantitative proof of the correctness of the line identifications. The identifications of Nakagawa *et al.*[5] are thereby confirmed.

The best previously determined value[5] of γ'' is 39 ± 6 MHz. It is only because the laser-rf double-resonance technique can measure γ'' with orders of magnitude more precision that the new behavior at small N can be observed.

Figure 6 shows the corresponding plot of $\langle\Delta\nu\rangle$ versus N. Here we see not a constant, but a varying function with a clear maximum at $N=11-12$ (see also Table II). Although the hyperfine splittings of the $J''=N+\frac{1}{2}$ and $N-\frac{1}{2}$ $^2\Sigma$ levels could not be determined individually by the present rf techniques because of the very small transition probabilities involved, the splitting of the $P_1(J'')$ and $Q_{12}(J'')$ lines could be observed by laser fluorescence as seen, for example, in Fig. 2. Because of the possibility of a small $^2\Pi_{1/2}$ hfs, the splittings of the $P_1(J'')$ and $Q_{12}(J'')$ lines might be slightly different from the splittings of the $J''=N\pm\frac{1}{2}$ $^2\Sigma$ levels. Although it was difficult to obtain quantitative measurements of the splittings of the fluorescence lines, rough values were obtained. The Q_{12} splitting was found to be very large (>60 MHz) at small J'' and to approach an asymp-

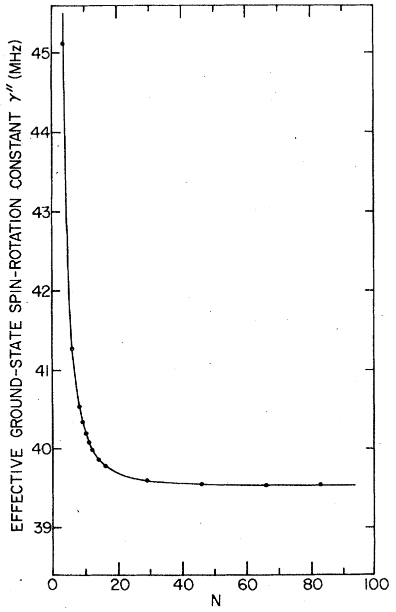

FIG. 5. Plot of the effective spin-rotation-interaction constant γ'' measured for the $v''=0$ $^2\Sigma$ ground state as a function of N, the rotational quantum number. The strong departure of γ'' at small N from its asymptotic value has not been observed before.

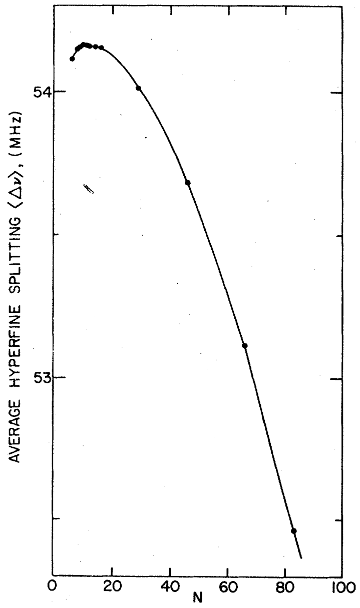

FIG. 6. Plot of the average hfs splitting ($\langle\Delta\nu\rangle$) measured for the $J''=N+\frac{1}{2}$ and $N-\frac{1}{2}$ levels as a function of N. The nonconstancy of this quantity is here observed for the first time.

tote of about 52 MHz for $J'' \gtrsim 80$, while the P_1 splitting was small at very small J'' (<40 MHz) and to approach approximately the same asymptotic value for $J'' \gtrsim 80$.

VI. INTERPRETATION AND CONCLUSIONS

A detailed comparison of the present experimental results with the theory, including the N dependence of γ'' and $\langle \Delta\nu \rangle$, will be published separately.[13] Although the new results have not been explicitly predicted by the basic theory, they are consistent with it.

The theoretical analysis[13] is based on the spin-rotation[15] and hyperfine[16] Hamiltonians, which may be combined as

$$\mathcal{H}_{\mathrm{SR,hfs}} = \gamma_{vN}\vec{S}\cdot\vec{N} + C_{IvN}\vec{I}\cdot\vec{N} + b_{vN}\vec{I}\cdot\vec{S} + c_{vN}(\vec{I}\cdot\hat{k})(\vec{S}\cdot\hat{k}), \qquad (3)$$

in which $\vec{S}, \vec{I}$, and $\vec{N}$ are the electron spin, nuclear spin, and molecular rotational angular mementa, respectively, and $\hat{k}$ is a unit vector along the internuclear axis. The subscripts v and N on the parameters indicate that they are functions of the vibrational and rotational states considered.

The new data can be used to evaluate[13] the N dependence of the parameters for the first time. The strong N dependence of the average hfs splitting arises from competition between the two hfs terms in Eq. (3), $b_{vN}\vec{I}\cdot\vec{S}$ and $c_{vN}(\vec{I}\cdot\hat{k})(\vec{S}\cdot\hat{k})$. Their different N dependence leads to the striking result shown. The hyperfine structure results obtained previously from matrix-isolation spin-resonance studies[17] are within 2% of the present values.

The dramatic departure in the value of the effective spin-rotation constant γ'' at low N from its asymptotic value, on the other hand, is due to competition between the spin-rotation and hyperfine terms in Eq. (3), and the effect becomes especially severe at small N where the two splittings are comparable. In this region, the spin and rotational angular momenta become uncoupled.

Application of the new laser-rf double-resonance technique to the study of CaF has not only achieved enormously greater precision, but has thereby revealed new structural effects not previously seen or explicitly predicted. Application of the basic theory[13] to the problem has resulted in quantitative understanding of these new phenomena and, in the process provided, extremely good values of the underlying physical quantities for comparison with *ab initio* calculations. In addition, the experimental results and their theoretical interpretation have suggested further interesting areas of study in the CaF molecule, particularly with regard to evaluation of the vibrational dependence of the parameters in Eq. (3). The present work also strongly suggests that the same technique can be profitably used to study more complex molecules.

ACKNOWLEDGMENTS

The authors would like to express their sincere thanks to I. Renhorn for suggesting the application of the new technique to CaF, to G. Goodman for his great insight and helpfulness during and after the experimental stages, and to S. A. Lee for constructing the λ-meter which was absolutely essential for all phases of the experimental work. This work was performed under the auspices of the Division of Basic Energy Sciences of the U. S. Department of Energy.

---

[1] R. W. Field, A. D. English, T. Tanaka, D. O. Harris, and D. A. Jennings, J. Chem. Phys. 59, 2191 (1973).

[2] P. J. Domaille, T. C. Steimle, and D. O. Harris, J. Mol. Spectrosc. 65, 354 (1977).

[3] P. J. Domaille, T. C. Steimle, and D. O. Harris, J. Mol. Spectrosc. 68, 146 (1977).

[4] R. W. Field, D. O. Harris, and T. Tanaka, J. Mol. Spectrosc. 57, 107 (1975).

[5] J. Nakagawa, P. J. Domaille, T. C. Steimle, and D. O. Harris, J. Mol. Spectrosc. 70, 374 (1978).

[6] A. Adams, W. Klemperer, and J. M. Dunn, Can. J. Phys. 46, 2213 (1968).

[7] D. W. Green, Can. J. Phys. 49, 2552 (1971).

[8] S. D. Rosner, T. D. Gaily, and R. A. Holt, Phys. Rev. Lett. 35, 785 (1975).

[9] W. Ertmer and B. Hofer, Z. Phys. A276, 9 (1976).

[10] I. Renhorn (private communication).

[11] W. J. Childs, O. Poulsen, and L. S. Goodman, Phys. Rev. A 19, 160 (1979).

[12] The present instrument is a simplified version of that described in J. L. Hall and S. A. Lee, Appl. Phys. Lett. 29, 367 (1976).

[13] G. L. Goodman (unpublished).

[14] N. F. Ramsey, Phys. Rev. 76, 996 (1949).

[15] G. Herzberg, *Spectra of Diatomic Molecules* (Van Nostrand, New York, 1950).

[16] R. S. Frosch and H. M. Foley, Phys. Rev. 88, 1337 (1952).

[17] L. B. Knight, Jr., W. C. Easley, W. Weltner, Jr., and M. Wilson, J. Chem. Phys. 54, 322 (1971).